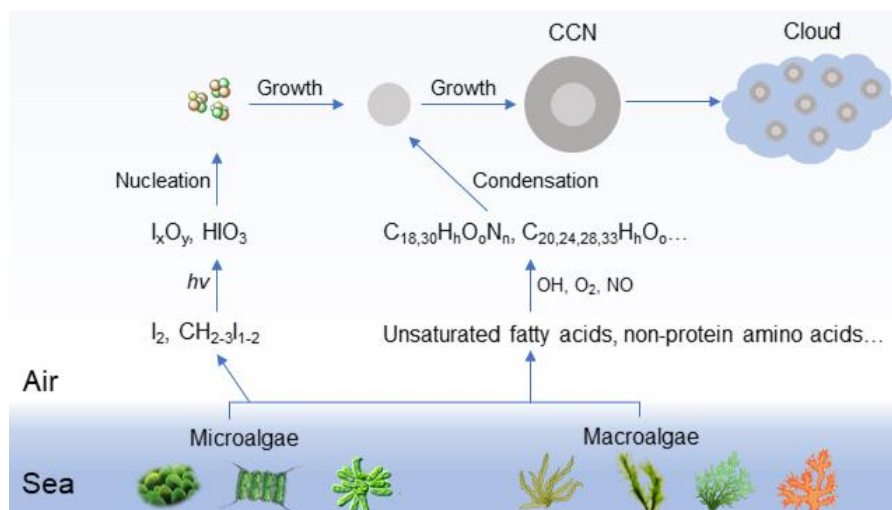




1 Probing key organic substances driving new particle growth initiated by  
2 iodine nucleation in coastal atmosphere  
3  
4 Yibei Wan,<sup>1</sup> Xiangpeng Huang,<sup>2</sup> Bin Jiang,<sup>3</sup> Binyu Kuang,<sup>4</sup> Manfei Lin,<sup>4</sup> Deming  
5 Xia<sup>5</sup>, Yuhong Liao,<sup>3</sup> Jingwen Chen,<sup>5</sup> Jianzhen Yu,<sup>4</sup> and Huan Yu<sup>1</sup>  
6 <sup>1</sup> Department of Atmospheric Science, School of Environmental Studies, China  
7 University of Geosciences, Wuhan, 430074, China  
8 <sup>2</sup> School of Environmental Science and Engineering, Nanjing University of Information  
9 Science and Technology, Nanjing, 210044, China  
10 <sup>3</sup> Guangzhou Institute of Geochemistry, Chinese Academy of Sciences, Guangzhou  
11 510640, China  
12 <sup>4</sup> Department of Chemistry, Hong Kong University of Science & Technology, Clear  
13 Water Bay, Kowloon, Hong Kong, China  
14 <sup>5</sup> School of Environmental Science and Technology, Dalian University of Technology,  
15 Dalian 116024, China  
16  
17 Corresponding author: H. Yu ([yuhuan@cug.edu.cn](mailto:yuhuan@cug.edu.cn))



## 18 Graphic abstract



19

## 20 ABSTRACT

21 Unlike the deep understanding of highly oxygenated organic molecules (HOMs)  
22 driving continental new particle formation (NPF), little is known about the organics  
23 involved in coastal and open ocean NPF. On the coastline of China we observed intense  
24 coastal NPF events initiated by iodine nucleation, but particle growth to cloud  
25 condensation nuclei (CCN) sizes was dominated by organic compounds. This article  
26 revealed a new group of  $C_{18,30}H_hO_oN_n$  and  $C_{20,24,28,33}H_hO_o$  compounds with specific  
27 double bond equivalents and oxygen atom numbers in sub-20 nm coastal iodine new  
28 particles by using ultrahigh resolution Fourier transform-ion cyclotron resonance mass  
29 spectrometry (FT-ICR-MS). We proposed these compounds are oxygenated or nitrated  
30 products of long chain unsaturated fatty acids, fatty alcohols, non-protein amino acids  
31 or amino alcohols emitted mutually with iodine from coastal biota or biological-active  
32 sea surface. Group contribution method estimated that the addition of  $-ONO_2$ ,  $-OH$  and  
33  $-C=O$  groups to the precursors reduced their volatility of by 2~7 orders of magnitude  
34 and thus made their products condensable onto iodine new particles in the coastal  
35 atmosphere. Non-target MS analysis also provided a list of 440 formulas of iodinated



36 organic compounds in size-resolved aerosol samples during the iodine NPF days, which  
37 facilitates the understanding of unknown aerosol chemistry of iodine.

## 38 1. INTRODUCTION

39 Atmospheric new particle formation (NPF) contributes over half of global cloud  
40 condensation nuclei (CCN) (Merikanto et al., 2009) and thus influences cloud  
41 properties and Earth's radiation budget (Metzger et al., 2010). By deploying high  
42 resolution Chemical Ionization Mass spectrometer, recent laboratory and field studies  
43 have identified a group of highly-oxidized organic molecules (HOMs) with high O/C  
44 ratio and extremely low volatility from the reactions of volatile organic compounds  
45 (VOCs) such as monoterpenes (Ehn et al., 2014). Sesquiterpenes (Richters et al., 2016)  
46 and alkene (Mentel et al., 2015) with hydroxyl radical (OH), ozone (O<sub>3</sub>) and nitrate  
47 radicals (NO<sub>3</sub>). These HOMs play an important role in particle nucleation and growth  
48 of continental NPF, as well as in the formation of secondary organic aerosols.

49 Unlike the deep understanding of continental HOMs, little is known about the role  
50 of organics in the NPF in coastal or open ocean atmosphere. The current state of  
51 knowledge is that the self-clustering of biogenic iodine oxides or oxoacids could initiate  
52 NPF events with particle number concentration sometimes exceeding 10<sup>6</sup> cm<sup>-3</sup> (O'Dowd  
53 et al., 2002; Burkholder et al., 2004; Sipilä et al., 2016; Stevanović et al., 2019; Kumar  
54 et al., 2018). But it is unknown if other species are needed to drive the growth of iodine  
55 clusters to CCN sizes in coastal or open ocean atmosphere (Saiz-Lopez et al., 2012).  
56 Iodine-induced NPF (I-NPF) events were mostly reported in European coastlines (Yoon  
57 et al., 2006; Mahajan et al., 2010) and polar regions (Allan et al., 2015; Roscoe et al.,  
58 2015; Dall'Osto et al., 2018). In 2019 we provided evidences of I-NPF in the southeast  
59 coastline of China, based on particle number size distribution and iodine measurements  
60 (Yu et al., 2019). The focus of that paper (Yu et al., 2019) is, however, the speciation  
61 of organic iodine compounds in size-segregated aerosol samples. Moreover, the use of  
62 relatively low resolution Time-of-Flight (TOF) mass analyzer and *in vitro* signal  
63 amplification approach in that paper did not allow the detection of the majority of non-



64 aromatic organic iodine compounds. Organic iodine remains to be the most significant  
65 unknown in aerosol iodine chemistry at present (Saiz-Lopez et al., 2012).

66 Fourier Transform Ion Cyclotron Resonance (FT-ICR) coupled with soft ionization  
67 techniques such as electrospray ionization (ESI) and ambient pressure chemical  
68 ionization (APCI) allows characterization of complex organic mixtures at the molecular  
69 level due to its ultra-high resolution and mass accuracy (Pratt and Prather, 2012). This  
70 technique has been used to examine molecular composition of organic aerosols (Schum  
71 et al., 2018; An et al., 2019; Zuth et al., 2018; Daellenbach et al., 2018; Xie et al., 2020)  
72 and cloud water (Zhao et al., 2013; Bianco et al., 2018). Studies investigating coastal  
73 organic aerosols have been rarely. Virtually no study reported the characterization of  
74 organic compounds driving the growth of coastal or open ocean new particles.

75 In this study, comprehensive chemical composition analyses were conducted on the  
76 size-segregated aerosol samples down to 10 nm, collected by 13-stage nano-MOUDI  
77 (nano-micro orifice uniform deposit impactor) during the intense I-NPF days at a  
78 coastal site of China. Relative abundances of  $\text{HSO}_4^-$ , total iodine and total organic  
79 carbon (TOC) in 10-56 nm particles were compared between the I-NPF days and  
80 conventional continental NPF days. In particular, using ultra-high resolution FT-ICR  
81 MS, we conducted a non-target analysis of particle-phase organic compounds to  
82 explore their molecular identity, formation mechanism and the role in new particle  
83 growth in the coastal atmosphere.

## 84 **2. METHDOLOGY**

### 85 **2.1. Sampling collection**

86 The sampling site (29°29' N, 121°46' E) is in a building about 40 and 200m away  
87 from the coastline of East China Sea (Zhejiang Province) at high tide and low tide,  
88 respectively. The classification of I-NPF event and continental regional NPF (C-NPF)  
89 event was based on particle number size distributions (PNSD) between 2 and 750 nm  
90 monitored from January to May 2018 by a scanning mobility particle spectrometer



91 (SMPS; TSI DMA3081 and CPC3775; scanning range: 40-750 nm) and a neutral  
92 cluster air ion spectrometer (NAIS; scanning range: 2-42 nm). Strong I-NPF events  
93 were observed almost every day in April and May, which was the growth and farming  
94 season of seaweed. A nano-MOUDI sampling scheme was implemented according to  
95 the PNSD measurement. One set of nano-MOUDI samples was collected during the C-  
96 NPF days from February 11 to 13; a second set was collected during the non-NPF days  
97 from April 16 to 18; a third set was collected during the I-NPF days from May 9 to 11.  
98 The PNSD during the 3 periods are shown in Figure S1. Each set of nano-MOUDI  
99 samples was collected continuously for 72 hours, during which NPF occurred on a daily  
100 basis, so that particle chemical composition of different event types can be obtained  
101 from offline analyses. Aluminum foil filters were used as sampling substrate to avoid  
102 the adsorption of gaseous species. For each set of nano-MOUDI samples, two nano-  
103 MOUDIs were placed side by side to collect 10-100 nm particles (on stages 10-13; other  
104 stages were silicon greased) and 100 nm-18  $\mu\text{m}$  particles (on stages 1-9) separately, in  
105 order to reduce potential positive particle-bounce artifacts. Three additional sets of  
106 blank samples were collected by placing a high efficiency particulate air (HEPA) filter  
107 at the gas inlet of nano-MOUDI. Detailed information on aerosol sample collection  
108 could be found in Yu et al. (2019).

## 109 **2.2. Sample preparation and analysis**

110 Half of each filter was transferred into a 20 mL tapered plastic centrifuge tube, added  
111 10 mL mixed solvent (1:1 v/v water and methanol; LCMS grade). The mixture was  
112 sonicated for 40 min and filtered by a 0.2  $\mu\text{m}$  PTFE membrane syringe filter. The filtrate  
113 was evaporated to almost dryness in a rotary evaporator below 40  $^{\circ}\text{C}$  and subsequently  
114 redissolved in 0.5 mL water. After being centrifuged for 30 min at 12,000 rpm, the  
115 supernatant was collected for total iodine (I) analysis by Agilent 7500a ICP-MS  
116 (Agilent Technologies, Santa Clara, CA, USA) and  $\text{HSO}_4^-$  analysis by UPLC-ESI-Q-  
117 TOF-MS. The measurements of  $\text{HSO}_4^-$  and total I were elaborated in our previous  
118 article Yu et al. 2019. Another half of each filter was extracted in the same way but  
119 used for TOC analysis by a TOC analyzer (Model TOC-5000A, Shimadzu, Japan) and



120 non-target MS analysis of organic compounds (OC) by ESI-FT-ICR-MS (SolariX XR  
121 9.4T instrument, Bruker Daltonics, Coventry, UK). Samples were infused by a syringe  
122 pump and analyzed in both positive (ESI+) and negative (ESI-) modes. ESI-FT-ICR  
123 MS operation conditions are included in Supplement Material. Field blank sample  
124 extracts were analyzed following the same procedure.

125

### 126 **2.3. FT-ICR MS data processing**

127 A resolving power ( $m/\Delta m_{50\%}$ ) 550,000 at  $m/z$  300 of our FT-ICR-MS allows the  
128 determination of possible formulas for singly charged molecular ions. Only  $m/z$  values  
129 between 150-1000 Da that satisfies signal/noise (S/N) ratio  $> 10$  were considered. For  
130 each  $m/z$  value, several scientific rules were applied to calculate a reasonable elemental  
131 formula of natural organic molecule: the general formula is  $C_{1-50}H_{1-100}O_{0-50}N_{0-10}I_{0-3}$  in  
132 the ESI+ mode; elemental ratios H/C, O/C, and N/C are limited to 0.3-3, 0-3 and 0-1.3,  
133 respectively. The general formula is  $C_{1-50}H_{1-100}O_{1-50}N_{0-5}S_{0-2}I_{0-3}$  in the ESI- mode;  
134 elemental ratios H/C, O/C, N/C and S/C are limited to 0.3-3, 0-3, 0-0.5 and 0-0.2,  
135 respectively. Mass error must be smaller than 0.5 ppm. Formula containing C, H, O, N,  
136 S and I isotopologues were removed from the formula lists. A formula with  $m/z > 500$   
137 was not reported if it did not belong to any  $CH_2$  homologous series. For a formula  
138  $C_cH_hO_oN_nS_sI_x$ , double bond equivalents (DBE) defined as  $DBE = \frac{2c+2-h+n-x}{2}$  was  
139 required to be non-negative. Formula calculation was done following the same  
140 procedure for the three field blank samples. All formulas found in the field blank  
141 samples, regardless of peak intensity, were excluded from the formula lists of real  
142 samples. Aromaticity index (AI) is calculated from  $AI = \frac{DBE_{AI}}{C_{AI}} = \frac{1+c-o-s-0.5h}{c-o-s-n}$ . If  
143  $DBE_{AI} \leq 0$  or  $C_{AI} \leq 0$ , then  $AI = 0$ . A threshold value of  $AI \geq 0.5$  provides an  
144 unambiguous minimum criterion for the presence of aromatic structure in a  
145 molecule (Yassine et al., 2014).



146 **3. RESULTS AND DISCUSSION**

147 **3.1. Organics dominate the growth of new particles initiated by iodine nucleation**

148 We first compare relative concentrations of major aerosol components, that is, total  
149 I,  $\text{HSO}_4^-$  and TOC, in nano-meter new particles during different event days. Total I  
150 ( $13.5 \text{ ng m}^{-3}$ , Table 1) in 10-56 nm particles during the I-NPF days was 67 and 36 times  
151 higher than those during the C-NPF days ( $0.2 \text{ ng m}^{-3}$ ) and non-event days ( $0.37 \text{ ng m}^{-3}$ ).  
152 In the same size range,  $\text{HSO}_4^-$  concentration ( $0.2 \text{ } \mu\text{g m}^{-3}$ ) during the I-NPF days was  
153 lower than that during the C-NPF days ( $0.5 \text{ } \mu\text{g m}^{-3}$ ). This clearly indicates that the NPF  
154 events from May 9 to 11 was linked to iodine nucleation. Even so, aerosol mass in 10-  
155 56 nm new particles during the I-NPF days was dominated by organics. We define the  
156 mass fraction of organic mass (OM) in the particles as  $(1.5m_{\text{TOC}})/(m_{\text{Total I}} + m_{\text{HSO}_4^-} +$   
157  $1.5m_{\text{TOC}}) \times 100\%$  by assuming a OM/TOC ratio of 1.5. Mass fractions of OM are 95%,  
158 87% and 68%, respectively, in the size bins 10-18 nm, 18-32 nm and 32-56 nm during  
159 the I-NPF days. Therefore, organic compounds are critical for I-NPF to contribute to  
160 CCN. The main purpose of this article is to identify these organic compounds during  
161 the I-NPF days. The OC composition during the C-NPF days is beyond the scope of  
162 this article.

163

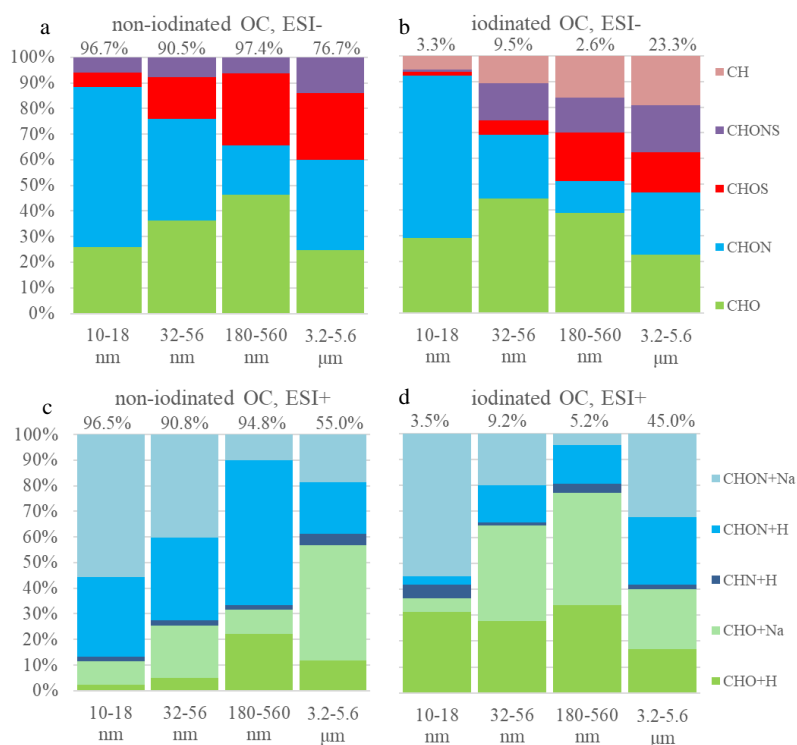
164 Table 1. Concentrations of Total iodine (I),  $\text{HSO}_4^-$  and Total Organic Carbon (TOC)  
165 in 3 size bins between 10-56 nm during the I-NPF, C-NPF and non-NPF days. For  
166 simplicity, only the sum of three size bins are shown for the C-NPF and non-NPF  
167 days. BDL=below detection limit.

	I-NPF			C-NPF	non-NPF
	10-18 nm	18-32 nm	32-56 nm	10-56 nm	10-56 nm
Total I ( $\text{ng m}^{-3}$ )	2.3	6.2	5.0	0.20	0.37
$\text{HSO}_4^-$ ( $\mu\text{g m}^{-3}$ )	0.022	0.034	0.144	0.50	BDL
TOC ( $\mu\text{g m}^{-3}$ )	0.31	0.18	0.21	0.28	BDL



### 168 3.2. Elemental composition of non-iodinated OC on the I-NPF days

169 Non-target analysis of OC elemental composition was performed in detail on 10-18  
170 nm, 32-56 nm, 180-560 nm and 3.2-5.6  $\mu\text{m}$  particles during the I-NPF days. Elemental  
171 formulas in the 4 size bins can represent OC molecular composition of nucleation mode,  
172 Aitken mode, accumulation mode and coarse mode, respectively. OC formulas were  
173 divided into two categories: non-iodinated OC and iodinated OC. There are far more  
174 non-iodinated OC formulas than iodinated OC formulas in  $<1 \mu\text{m}$  particles in terms of  
175 both formula number (Table 2) and relative intensity (Figure 1). For example, 2831  
176 non-iodinated OC formulas account for 96.6% of OC total intensity in 10-18 nm  
177 particles, while 137 iodinated OC formulas account for the remaining 3.4%. It means  
178 that non-iodinated OC dominates new particle growth during the I-NPF events. In this  
179 section, we first discuss chemical characteristics of non-iodinated OC, while the  
180 speciation of iodinated OC will be discussed in Section 3.4.







182 Figure 1. Relative intensity distributions of elemental groups observed in 10-18 nm, 32-  
183 56 nm, 180-560 nm and 3.2-5.6  $\mu\text{m}$  size bins in ESI+ and ESI- modes. The percentage  
184 above a column denote the percent of non-iodinated OC (or iodinated OC) intensity in  
185 total OC intensity in a size bin. +Na and +H denote  $[\text{M}+\text{Na}]^+$  and  $[\text{M}+\text{H}]^+$  adduct in  
186 ESI+ mode, respectively.

187 The molecular formulas of non-iodinated OC were divided into seven elemental  
188 groups  $\text{CHO}^-$ ,  $\text{CHO}^+$ ,  $\text{CHON}^-$ ,  $\text{CHON}^+$ ,  $\text{CHOS}^-$ ,  $\text{CHONS}^-$  and  $\text{CHN}^+$ . The number  
189 distribution of 7 elemental groups for the 4 size bins is listed in Table 2. If both  $[\text{M}+\text{Na}]^+$   
190 and  $[\text{M}+\text{H}]^+$  adducts of a formula were detected, the formula was counted only once. It  
191 should be noted that some formulas were repeatedly detected in ESI+ and ESI- modes.  
192 Some formulas detected in one size bin were also detected in another size bin. This is  
193 quantitatively shown in the first four rows of Table 2. For instance, 58%, 25% and 4%  
194 of the formulas detected in 10-18 nm aerosols were also detected in 32-56 nm, 180-560  
195 nm and 3.2-5.6  $\mu\text{m}$  aerosols, respectively. In another word, the particles in neighboring  
196 size bins share more similarity in organic composition. An unexpected finding is that  
197 the number of non-iodinated OC formulas detected in 3.2-5.6  $\mu\text{m}$  coarse particles ( $n =$   
198 266) is one order of magnitude lower than those of other bins. Reconstructed mass  
199 spectra of the 7 elemental groups in ESI- and ESI+ modes are shown in Figure S2 for  
200 the four size bins.

201

202 Table 2. The numbers of assigned formulas of elemental groups of organic compounds  
203 in 10-18 nm, 32-56 nm, 180-560 nm and 3.2-5.6  $\mu\text{m}$  size bins. The first 4 rows show  
204 the percent of formula repeatability between two size bins. 1I-OC: molecular formula  
205 containing one iodine atom.

Repeatability	10-18 nm	32-56 nm	180-560 nm	3.2-5.6 $\mu\text{m}$	
10-18 nm		58%	25%	4%	
32-56 nm	57%		38%	4%	
180-560 nm	34%	51%		6%	
3.2-5.6 $\mu\text{m}$	35%	35%	34%		
Non-iodinated OC				Total	
$\text{CHO}^-$	531	565	525	20	892
$\text{CHO}^+$	250	501	380	111	857



CHON <sup>-</sup>	1005	638	347	25	1268	
CHON <sup>+</sup>	1139	1055	828	72	2121	
CHOS <sup>-</sup>	147	216	256	22	357	
CHONS <sup>-</sup>	134	131	93	10	259	
CHN <sup>+</sup>	34	26	7	7	46	
Total	2831	2770	2151	266	4979	
Iodinated OC					Total	II-OC (%)
CHOI <sup>-</sup>	32	53	11	5	80	64%
CHOI <sup>+</sup>	17	85	31	31	136	93%
CHONI <sup>-</sup>	52	29	7	7	77	88%
CHONI <sup>+</sup>	34	57	18	52	132	81%
CHOSI <sup>-</sup>	3	8	7	3	18	72%
CHONSI <sup>-</sup>	2	7	3	2	13	62%
CHNI <sup>+</sup>	6	4	4	3	16	56%
CHI <sup>-</sup>	4	2	1	4	9	67%
Total	137	228	76	100	440	80%

206 CHON is the most commonly assigned elemental group in both ESI+ (2121 CHON<sup>+</sup>)  
207 and ESI- (1268 CHON<sup>-</sup>) modes, followed by the CHO group (857 CHO<sup>+</sup> formulas and  
208 892 CHO<sup>-</sup> formulas). S-containing formulas are 357 CHOS<sup>-</sup> and 259 CHONS<sup>-</sup>. The  
209 formula number of the least common CHN<sup>+</sup> group is only 46. In terms of relative  
210 intensity, CHON fraction in the ESI- mode decreases from 61% of OC in the 10-18 nm  
211 bin to 20% in the 180-560 nm bin (Figure 1a), while the fractions of CHO and  
212 CHOS/CHONS increase with particle size. In the ESI+ mode, the fraction of CHON  
213 decreases from 88% in 10-18 nm bin to 70% in 180-560 nm bin, being always the  
214 dominant elemental group of non-iodinated OC (Figure 1b). Low molecular weight  
215 (LMW) amines are important stabilizers in acid-base nucleation (Kurtén et al., 2008;  
216 Jen et al., 2014; Zheng et al., 2000; Yao et al., 2016), but their molecular ions are out  
217 of the mass range of our FT-ICR-MS. The CHN<sup>+</sup> formulas that we observed contained  
218 9-50 C atoms and 1-7 N atoms, accounting for a negligible fraction 1.7% of total  
219 intensity of all ESI+ formulas in the 10-18 nm particles.

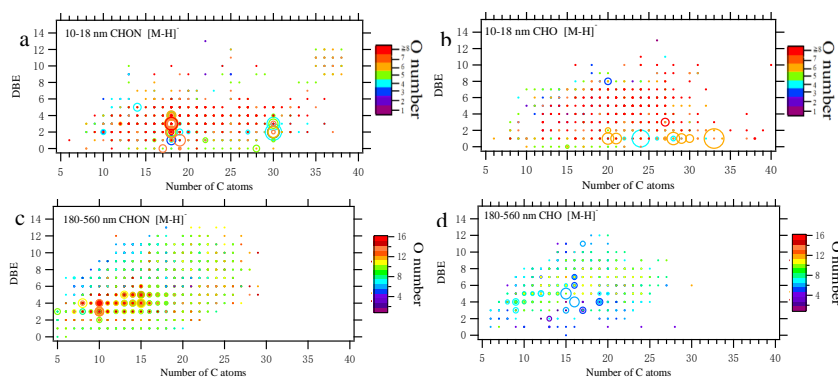
220 Previous elemental composition studies using FT-ICR-MS were mostly conducted  
221 on PM<sub>2.5</sub> or PM<sub>10</sub> collected from marine (Schmitt-Kopplin et al., 2012; Bao et al., 2018;  
222 Ning et al., 2019), urban (Wu et al., 2019; Jiang et al., 2016), troposphere (Schum et al.,  
223 2018; Mazzoleni et al., 2012) and forest sites (Kourtschev et al., 2013). In general, these  
224 studies showed that the numbers of CHO compounds were comparable with or more



225 than those of CHON compounds. Our study shows clearly that elemental composition  
226 of aerosol OC is highly size dependent. New particle growth in the size range of 10-18  
227 nm during the I-NPF event is dominated by CHON elemental group, followed by CHO.  
228 The focus of this article narrows on the identity and source of the CHON and CHO  
229 formulas in 10-18 nm particles, by comparing with those in the 180-560 nm size bin.  
230

### 231 3.2.1. CHO formulas

232 There is a total of 531 CHO<sup>-</sup> formulas and 250 CHO<sup>+</sup> formulas in 10-18 nm particles.  
233 54 CHO formulas are commonly found in ESI+ and ESI- modes. In terms of relative  
234 intensity, CHO<sup>-</sup> compounds are more abundant than CHO<sup>+</sup> compounds (Figure 3b, total  
235 intensity: 4.14 e+09 vs. 1.24 e+09). However, this is not indicative of absolute  
236 concentration of the two groups due to different ionization efficiency between ESI- and  
237 ESI+ modes. CHO<sup>-</sup> is characterized by a series of formulas with 20, 24, 28, and 33 C  
238 atoms, 4 or 6 O atoms and 1 equivalent double bond (Figure 2b). The total intensity of  
239 top 10 formulas accounts for 30% of all 531 formulas. Assuming CHO<sup>-</sup> formulas  
240 contain at least 1 carboxylic group (-COOH), the rest of their molecules should be  
241 saturated (DBE = 0) and contain 2 or 4 O atoms.  
242



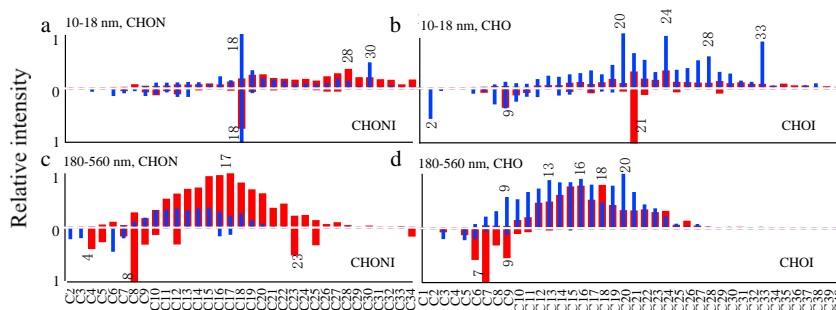
243  
244 Figure 2. DBE vs. C atom number diagrams of all CHON and CHO formulas detected  
245 in 10-18 nm and 180-560 nm particles in ESI- mode. The color bar denotes O atom



246 number in the formulas. The size of the circles reflects the relative intensities of  
247 molecular formulas on a logarithmic scale.

248

249 The above feature is not seen in either  $\text{CHO}^+$  formulas in the 10-18 nm bin or  $\text{CHO}^-$   
250 formulas in the 180-560 nm bin. There are more  $\text{C}_{21}$  and  $\text{C}_{24}$  formulas than other C  
251 subgroups in the  $\text{CHO}^+$  formulas of 10-18 nm bin (Figure S3d), but none of them have  
252 exceptionally-high intensity. The prominent formulas in the  $\text{CHO}^-$  group in 180-560  
253 nm particles have relatively high unsaturation degree ( $\text{DBE} = 3-7$ , Figure 2d). The  
254 relative intensities of subgroups according to C atom number in the  $\text{CHO}^-$  formulas in  
255 the 180-560 nm bin are characterized by bimodal distribution with maximum intensity  
256 around  $\text{C}_{15}-\text{C}_{16}$  and  $\text{C}_{20}$  (Figure 3d). The relative intensity of O atom subgroups is  
257 mono-modally distributed around  $\text{O}_7$  (Figure S4).



258

259 Figure 3. Relative intensities of subgroups according to C atom number in CHON, CHO,  
260 CHONI and CHOI formulas in 10-18 nm and 180-560 nm particles in ESI+ (in red) and  
261 ESI- (in blue). The intensity of the most abundant subgroup in a size bin is defined as  
262 1 and those of other subgroups are normalized by it. The relative intensities of non-  
263 iodinated OC formulas (iodinated OC formulas) are plotted in the region above (below)  
264 zero line.

265

### 266 3.2.2. CHON formulas

267 As discussed earlier, CHON is the most abundant elemental group observed in the  
268 smallest size bin 10-18 nm. There is a total of 1005  $\text{CHON}^-$  formulas (total intensity



269 9.96 e+09) and 1139 CHON<sup>+</sup> formulas (6.45 e+09) in 10-18 nm bin. 355 CHON  
270 formulas are commonly found in ESI<sup>+</sup> and ESI<sup>-</sup> modes. A close examination of Figure  
271 2a and 3a reveals that CHON<sup>-</sup> is characterized by a series of C<sub>18</sub> and C<sub>30</sub> formulas with  
272 low DBE values (1-4). 87 C<sub>18</sub> and 26 C<sub>30</sub> formulas account for 37% of total intensity of  
273 CHON<sup>-</sup>. Such feature is not seen for CHON<sup>+</sup> formulas that are rather uniformly  
274 distributed in DBE vs. C diagram (Figure S3a and S3c). Generally speaking, CHON<sup>-</sup>  
275 compounds should contain nitro- (-NO<sub>2</sub>) or nitrooxy- (-ONO<sub>2</sub>) group and are ionizable  
276 due to the presence of -COOH or hydroxy (-OH) (Lin et al., 2012). However, the  
277 presence of amine group in CHON<sup>-</sup> formulas cannot be excluded. Take C<sub>18</sub> as example,  
278 51 out of 87 C<sub>18</sub>H<sub>h</sub>O<sub>o</sub>N<sub>n</sub><sup>-</sup> formulas should contain at least one amine group, either  
279 because their O atom numbers are not large enough to allow the assignment of -NO<sub>2</sub>  
280 for all N atoms, or because some formulas (25 out of 87) were also detected in ESI<sup>+</sup>  
281 mode. In total, 51 C<sub>18</sub>H<sub>h</sub>O<sub>o</sub>N<sub>n</sub><sup>-</sup> formulas with an amine group account for 54.4% of total  
282 intensity of 87 C<sub>18</sub>H<sub>h</sub>O<sub>o</sub>N<sub>n</sub><sup>-</sup> formulas.

283 The presence of amine group in C<sub>18</sub>H<sub>h</sub>O<sub>o</sub>N<sub>n</sub><sup>-</sup> formulas in 10-18 nm particles is also  
284 supported by the comparison with CHON<sup>-</sup> in 180-560 nm submicron aerosols. CHON<sup>-</sup>  
285 in 180-560 nm is characterized by a number of formulas with maximum intensity  
286 around C<sub>10</sub> and C<sub>15</sub> (Figure 2c). A plot of O atom number vs. N atom number in Figure  
287 S5a shows that C<sub>10</sub>H<sub>h</sub>O<sub>o</sub>N<sub>n</sub><sup>-</sup> in 180-560 nm have O/N ratios ≥ 3 and O atom number is  
288 positively correlated with N atom number. It indicates that these C<sub>10</sub>H<sub>h</sub>O<sub>o</sub>N<sub>n</sub><sup>-</sup> formulas  
289 are probably nitro- or nitrooxy- oxidation products of monoterpenes from continental  
290 plant emission. In contrast, O/N ratios of the C<sub>18</sub>H<sub>h</sub>O<sub>o</sub>N<sub>n</sub><sup>-</sup> formulas in 10-18 nm are  
291 mostly small and O atom number do not increase with N atom number (Figure S5b).  
292 All collective evidences above reveal that nitrogen-containing organic compounds in  
293 10-18 nm particles during the I-NPF days are partly composed of long-chain amino  
294 alcohols, amino acids and so on.

295 In summary, a series of very distinctive CHON<sup>-</sup> and CHO<sup>-</sup> formulas was observed in  
296 10-18 nm new particles during the I-NPF days. These formulas are characterized by  
297 some specific numbers of C atoms (i.e. C<sub>18</sub>H<sub>h</sub>O<sub>o</sub>N<sub>n</sub>, C<sub>30</sub>H<sub>h</sub>O<sub>o</sub>N<sub>n</sub>, C<sub>20</sub>H<sub>h</sub>O<sub>o</sub>, C<sub>24</sub>H<sub>h</sub>O<sub>o</sub>,  
298 C<sub>28</sub>H<sub>h</sub>O<sub>o</sub> and C<sub>33</sub>H<sub>h</sub>O<sub>o</sub>) and equivalent double bonds (DBE = 1 for CHO<sup>-</sup> and 1-4 for



299 CHON<sup>-</sup>). To the best of our knowledge, such CHON<sup>-</sup> and CHO<sup>-</sup> formulas have not been  
300 reported by previous aerosol studies. The chemical composition of new particles is  
301 completely decoupled with the CHO<sup>-</sup> and CHON<sup>-</sup> formulas around C<sub>10</sub>, C<sub>15</sub> and C<sub>20</sub> in  
302 180-560 nm submicron particles, which might be originated from continental terpene  
303 emissions. Fewer O atoms in C<sub>18,30</sub>H<sub>h</sub>O<sub>o</sub>N<sub>n</sub> and C<sub>20,24,28,33</sub>H<sub>h</sub>O<sub>o</sub> formulas than those in  
304 submicron aerosols indicate that these compounds should be more freshly emitted into  
305 the atmosphere. The discontinuous chemical composition and PNSD spectrum (Figure  
306 S1a) below and above 50 nm particle size reflect the fact that the further growth of new  
307 particles beyond 50 nm in local I-NPF events cannot be monitored by our stationary  
308 sampling strategy.

309 On the other hand, we observed more complicated distributions of CHO<sup>+</sup> and  
310 CHON<sup>+</sup> formulas in 10-18 nm new particles that are of relatively small individual  
311 intensity and are rather uniformly distributed in DBE vs. C diagrams. Like CHON<sup>-</sup> and  
312 CHO<sup>-</sup>, those CHO<sup>+</sup> and CHON<sup>+</sup> formulas also possess a larger number of C atoms (C >  
313 19) than their counterparts in 180-560 nm submicron aerosols (Figure 3). 21 out of 30  
314 most abundant CHON<sup>+</sup> formulas contain two or more N atoms; this ratio 21/30 is higher  
315 than those in CHON<sup>-</sup> formulas. Generally speaking, CHO<sup>+</sup> and CHON<sup>+</sup> formulas  
316 represent carbonyls/alcohols/epoxides and amino alcohols/amino acids, respectively.  
317 One interesting finding about CHO<sup>+</sup> and CHON<sup>+</sup> is that they tend to form [M+Na]<sup>+</sup>  
318 adducts in small aerosols and [M+H]<sup>+</sup> adducts in large aerosols (Figure 1c). This  
319 indicates that the CHO<sup>+</sup> and CHON<sup>+</sup> compounds in new particles during the I-NPF days  
320 should possess different basic functional groups from those in submicron particles.

### 321 3.3. Possible precursors and formation mechanism of organic compounds

#### 322 detected in 10-18 nm new particles during the I-NPF days

323 It is unrealistic to simply propose one out of a large number of possible structures for  
324 a formula with large C atom number (e.g., ≥ 18). Our strategy is to first explore the  
325 possible precursors of the newly found CHON and CHO formulas. It is obvious that  
326 these C<sub>18,30</sub>H<sub>h</sub>O<sub>o</sub>N<sub>n</sub> and C<sub>20,24,28,33</sub>H<sub>h</sub>O<sub>o</sub> formulas cannot be attributed to continental



327 terpene emission or anthropogenic aromatic emissions. Previous field measurements of  
328 marine NPF precursor focused on volatile species like iodine (Stevanović et al., 2019),  
329 iodomethanes (O'Dowd et al., 2002), dimethyl sulfonic acid (Yvon et al., 1996; Barone  
330 et al., 1996; Barnes et al., 2006) and LMW amines (Ning et al., 2019; Ge et al., 2011).  
331 So far there is no report about aliphatic compounds with C number  $\geq 18$  in either gas  
332 phase or new particles (Cochran et al., 2017; Bikkina et al., 2019). Therefore, we  
333 consulted the literature that reported chemical compounds isolated from biological  
334 tissues of algae, plankton or other marine organisms. Potential precursors are listed in  
335 Table 3.

### 336 3.3.1. Fatty acids

337 Fatty acids (FAs) are widely found in animals, plants and microbe (Moss et al., 1995).  
338 Plants have higher content of unsaturated FAs than animals.  $C_{14}$ - $C_{24}$  fatty acids,  
339 including both saturated and unsaturated, have long been observed in seaweed  
340 (Dawczynski et al., 2007) and very long chain FAs ( $C_{24}$ - $C_{36}$ ) have been isolated from  
341 green algae, *Chlorella kessleri*, sponges and marine dinoflagellate (Litchfield et al., 1976;  
342 Řezanka and Podojil, 1984; Mansour et al., 1999).  $C_{18}$  Oleic acid, linoleic acid and  
343 linolenic acid are most commonly found unsaturated FAs in macro algae. FAs with  
344 carbon chain shorter than  $C_{20}$  were used by atmospheric chemists as organic tracers of  
345 atmospheric aerosols from microbe or kitchen emission (Simoneit and Mazurek, 1982;  
346 Zheng et al., 2000; Guo et al., 2003; Rogge et al., 1991; DeMott et al., 2018;  
347 Willoughby et al., 2016). In our study, no saturated FAs were detected in 10-18 nm  
348 particles. Only 1.5% CHO<sup>-</sup> formulas can be assigned to unsaturated FAs (that is, include  
349 2 O atoms, 14-28 C atoms and DBE = 3-6). Other CHO compounds observed in 10-18  
350 nm particles contain  $> 2$  O atoms and thus can be assigned as the oxidized derivatives  
351 of FAs.

352

353 Table 3 Possible precursors and their presence in marine biological sources and our  
354 aerosol samples. ND: not detected.

Potential precursors	Presence in marine sources	Presence in aerosol particles
----------------------	----------------------------	-------------------------------



Unsaturated fatty acid	C <sub>14</sub> -C <sub>24</sub> fatty acids	Seaweed (Dawczynski et al., 2007)	1.5% of CHO in terms of relative intensity
	C <sub>25</sub> --C <sub>36</sub> very long chain fatty acids	Green algae, chlorella kessleri, sponges, marine dinoflagellate (Litchfield et al., 1976; Řezanka and Podojil, 1984; Mansour et al., 1999).	ND
fatty alcohols	C <sub>30</sub> -C <sub>32</sub> mono- and diunsaturated alcohols and diols	Yellow-green algae (Volkman et al., 1992)(eustigmatophytes)	ND
Saturated hydroxyl fatty acids	C <sub>20</sub> H <sub>40</sub> O <sub>3</sub> , C <sub>32</sub> H <sub>64</sub> O <sub>4</sub>	Nannochloropsis, cutins and suberins of higher plants (Gelin et al., 1997).	S/N 15 and 28
Nonprotein amino acid	C <sub>18</sub> H <sub>37</sub> NO <sub>4</sub> saturated dihydroxy amino acid (simplifungin,		S/N 280
	C <sub>20-22</sub> H <sub>39-41</sub> NO <sub>5-7</sub> mono-unsaturated polyhydroxy amino acids in sphingolipids	Marine fungal metabolites (Ishijima et al., 2016; VanMiddlesworth et al., 1992).	S/N 30-230
Amino alcohols	C <sub>16-28</sub> H <sub>33-53</sub> NO <sub>1-4</sub> polyhydroxy amino alcohols	Plant biomembrane, secondary metabolites in marine organisms (Jares-Erijman et al., 1993).	S/N 23-640
	C <sub>18</sub> H <sub>31</sub> NO and C <sub>18</sub> H <sub>29</sub> NO polyunsaturated amino alcohols	Mediterranean tunicate (Jares-Erijman et al., 1993)	S/N 10-60
	C <sub>18</sub> H <sub>36</sub> N <sub>2</sub> O <sub>5</sub> polyhydroxy cyclic alkaloid	Moraceae (Tsukamoto et al., 2001)	S/N 800

355

356 Possible oxidation schemes of two typical C<sub>18</sub> (C<sub>18</sub>H<sub>30</sub>O<sub>2</sub>,  $\alpha$ -linolenic acid, three C=C  
 357 double bonds in carbon chain) and C<sub>28</sub> unsaturated FAs (C<sub>28</sub>H<sub>52</sub>O<sub>2</sub>, two C=C double  
 358 bonds), for instance, are proposed in Figure S6 and S7. The reaction of an unsaturated  
 359 FA after the emission into the atmosphere is initiated by OH addition to C=C double  
 360 bond and subsequent O<sub>2</sub> addition to form a peroxy radical (Atkinson et al., 1995;  
 361 Calvert et al., 2000). Depending on the level of NO and reactivity, four competitive  
 362 pathways are available for peroxy radicals to produce CHO or CHON formulas  
 363 observed in our study: reaction with NO to form a -ONO<sub>2</sub> group (pathway 1) or an  
 364 alkoxy radical that further reacts with O<sub>2</sub> to form a carbonyl (-C=O, pathway 2),  
 365 reaction with RO<sub>2</sub> radicals to form a hydroxyl (-OH) or a -C=O group (pathway 3) and  
 366 successive intermolecular H-shift/O<sub>2</sub> addition autoxidation(Crouse et al., 2013;  
 367 Vereecken et al., 2015) (pathway 4).

368 We propose that pathway 1 and 2 are preferred for those FAs (e.g.,  $\alpha$ -linolenic acid)  
 369 with higher reactivity with NO (Figure S6). Pathways 1 and 2 add -ONO<sub>2</sub>, -OH and -  
 370 C=O groups to carbon chain but do not reduce the DBE of FA precursor.  $\alpha$ -linolenic  
 371 acid oxidation in the atmosphere via sequential occurrences of pathways 1 or 2 yields





372 a series of oxygenated and nitrated organic compounds, among which  $C_{18}H_{31}NO_6$ ,  
373  $C_{18}H_{31}NO_8$ ,  $C_{18}H_{31}NO_{10}$ ,  $C_{18}H_{32}N_2O_{10}$  and  $C_{18}H_{33}N_3O_4$  are found in 10-18 nm particles.  
374 These formulas explain the circles with DBE = 4 and C number = 18 shown in Figure  
375 2a DBE vs. C atom number diagram.

376 We propose that pathway 3 and 4 are preferred for those FAs (e.g.  $C_{28}$  FA  $C_{28}H_{52}O_2$ )  
377 with higher reactivity with  $RO_2$  (Figure S7). The net outcome of sequential pathway 3  
378 and 4 reactions is to add  $-OH$  and  $-C=O$  groups and reduce the DBE of FA precursor.  
379 The end products are a series of  $C_{28}H_{52}O_{6-8}$ ,  $C_{28}H_{54}O_{4-7}$  and  $C_{28}H_{56}O_{6-8}$  compounds,  
380 which can explain the circles with C number = 28 and DBE = 1-3 in Figure 2b.

381 In addition to fatty acids, fatty alcohols such as  $C_{30}$ - $C_{32}$  mono- and di-unsaturated  
382 alcohols and diols have been detected in yellow-green algae (Volkman et al., 1992).  
383 Although these unsaturated alcohols were not detected in our 10-18 nm particles, we  
384 suppose that they or their metabolites in algae may undergo similar reactions like  
385 unsaturated FA to generate condensable oxygenated and nitrated fatty alcohols in the  
386 atmosphere. Hydroxy fatty acids (HFAs) are important constituents of lipid in marine  
387 microalgae (Gelin et al., 1997), bacteria (Kim and Oh, 2013), seaweed (Kendel et al.,  
388 2013; Blokker et al., 1998) and leaf surface of higher plants (Pollard et al., 2008).  
389 Among them, two saturated HFAs  $C_{20}H_{40}O_3$  and  $C_{32}H_{64}O_4$  were found in our 10-18 nm  
390 aerosol sample with S/N ratios 15 and 28. However, because saturated hydroxy fatty  
391 acids are not oxidizable via the pathways proposed in our study, they are assumed  
392 unlikely to be precursors of other formulas observed in 10-18 nm particles.

### 393 **3.3.2. Nonprotein amino acids and amino alcohols**

394 Quantum chemical calculations have showed that amino acids like Glycine, Serine,  
395 and Threonine are potential participants in atmospheric nucleation via interaction with  
396 sulfuric acid (Elm et al., 2013; Ge et al., 2018; Li et al., 2020). However, we did not  
397 observe any of 20 essential amino acids in 10-18 nm in either ESI+ or ESI- modes. One  
398 reason may be that most of essential amino acids have molecular weight less than 150  
399 that is below mass scan range of our FT-ICR-MS.

400 There are a number of records in the literature about long chain non-protein amino  
401 acids or amino alcohols isolated from marine organisms or plant biomembrane



402 (Ishijima et al., 2016; VanMiddlesworth et al., 1992; Jares-Erijman et al., 1993;  
403 Tsukamoto et al., 2001). They include saturated dihydroxy amino acid ( $C_{18}H_{37}NO_4$ ,  
404 DBE = 1, simplifungin), monounsaturated polyhydroxy amino acids in sphingolipids  
405 ( $C_{20-22}H_{39-41}NO_{5-7}$ , DBE = 2-3), polyhydroxy amino alcohols ( $C_{16-28}H_{33-53}N_{1-2}O_{1-5}$ ,  
406 DBE = 1-3, sphingosine and its natural metabolites) and polyunsaturated amino  
407 alcohols ( $C_{18}H_{31}NO$  and  $C_{18}H_{29}NO$ , DBE = 4-5). All of these formulas were detected  
408 in 10-18 nm aerosols with S/N in the range of 10-800. More importantly, all those  
409 compounds that contain at least one amine group and one C=C double bond can be  
410 precursors of observed CHON formulas containing amine group via the pathways that  
411 we showed above. As an example, the oxidation scheme of an amino alcohol  $C_{18}H_{31}NO$   
412 with 4 C=C double bonds in carbon chain is illustrated in Figure S8.

413 Similar to  $C_{28}$  FA,  $C_{18}H_{31}NO$  undergoes successive intermolecular H-shift/ $O_2$   
414 additions to produce a series of  $RO_2$  radicals with hydroperoxyl group ( $-OOH$ ) in its  
415 carbon chain. The subsequent pathway 3 reactions, as well as the decomposition of  $-$   
416  $OOH$  groups, add  $-OH$  and  $-C=O$  groups in the carbon chain. Because  $C_{18}H_{31}NO$   
417 possesses as many as 4 C=C double bonds, sequential pathway 3 and 4 reactions  
418 produce a large number of oxidation products, among which 57 are found in the formula  
419 list detected in 10-18 nm particles (Figure S8). These products  $C_{18}H_{31}NO_{4-11,13}$ ,  
420  $C_{18}H_{33}NO_{4,6-10}$ ,  $C_{18}H_{35}NO_{5-9}$ ,  $C_{18}H_{37}NO_{7-12}$  and  $C_{18}H_{39}NO_{10-11}$  explain perfectly the  
421 presence of a series of formulas with C number = 18, DBE = 0-4 and a  $-NH_2$  group  
422 shown in Figure 2a.

### 423 3.3.3. Volatility estimation

424 Based on the reaction mechanisms proposed above, it is possible to estimate the  
425 volatility change from potential precursors to their oxidation products. First, from the  
426 list of elemental formulas detected in 10-18 nm particles, we select 49 formulas with  
427 high intensities, including 14  $CHON^-$  formulas with peak intensity  $> 1.00 \times 10^8$ , 23  
428  $CHON^+$  formulas with peak intensity  $> 3.00 \times 10^7$  and 12  $CHO^-$  formulas (DBE = 1)  
429 with peak intensities  $> 3.00 \times 10^7$ . Possible combinations of  $-COOH$ ,  $-ONO_2$ ,  $-C=O$ ,  
430 C=C double bond,  $-NH_2$  and  $-OH$  groups are searched for every formula obeying two  
431 simple rules:  $CHON^-$  and  $CHO^-$  formulas must possess a carboxyl or hydroxyl group;

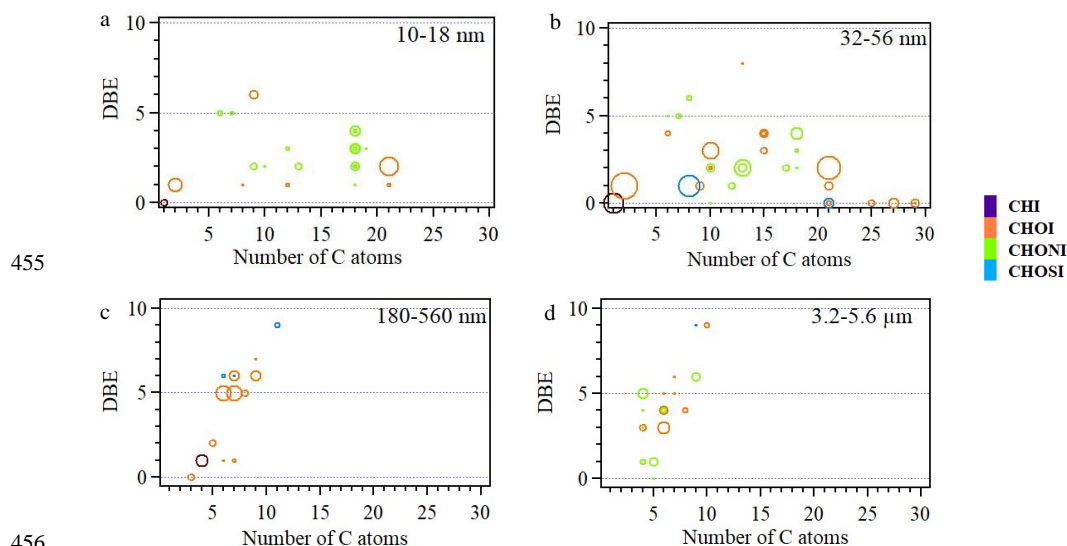


432 CHON<sup>+</sup> formulas must possess an amino group. Saturation concentrations (C\*) of the  
433 49 formulas were then predicted for all combinations using a simple group contribution  
434 method developed by Pankow and Asher (Pankow and Asher, 2008). On the other hand,  
435 the C\* of their possible precursors, including unsaturated FAs, fatty alcohols,  
436 nonprotein amino acids or amino alcohols, were predicted by the same method.

437 As we can see in Table S4, C\* of the 49 formulas fall into the range of ELVOC (< 3  
438 × 10<sup>-5</sup> μg m<sup>-3</sup>), while C\* of their precursors are in the range of SVOC (0.3-300 μg m<sup>-3</sup>)  
439 or LVOC (3 × 10<sup>-5</sup>-0.3 μg m<sup>-3</sup>). The addition of functional groups reduces the volatility  
440 of precursors by 2~7 orders of magnitude and thus make their oxidation products  
441 condensable onto new particles during the I-NPF event days. Therefore, the analysis of  
442 precursor-product volatility partly supports our hypothesis about the molecular identity  
443 and formation mechanism of the formulas detected in 10-18 nm particles.

#### 444 **3.4. Speciation of iodinated OC**

445 Organic iodine compounds hold the key to understand aerosol iodine chemistry and  
446 its role in regulating the recycling of halogens to the gas phase. We identified 440  
447 iodinated OC formulas from the 4 size bins during the I-NPF days (Table 2). 80% of  
448 the 440 formulas contain one I atom and the rest of them contain two I atoms. In terms  
449 of relative intensity, iodinated OC accounts for 2.6-9.5% of OC in fine particles, but its  
450 fraction in coarse particles increases to 23.3% in ESI- mode and 45% in ESI+ mode.  
451 The size distribution of 7 iodinated OC groups (i.e., CHOI<sup>-</sup>, CHONI<sup>-</sup>, CHOSI<sup>-</sup>,  
452 CHONSI<sup>-</sup>, CHOI<sup>+</sup>, CHONI<sup>+</sup> and CHNI<sup>+</sup>) resembles those of non-iodinated OC groups  
453 (Figure 1). If we replace I atom(s) with H atom(s) in a formula, 107 out of 440 replaced  
454 formulas are also found in the non-iodine OC formula list.



456  
457

458 Figure 4. DBE vs. C atom number diagrams of iodinated OC formulas with intensity >  
459 1.00 e+07 in the four size bins. The color bar denotes the elemental groups of assigned  
460 formulas. The size of the circles reflects the relative intensities of molecular formulas  
461 on a logarithmic scale.

462

463 Iodinated OC with intensity > 1.00 e+07 in the four size bins were shown in Figure  
464 4. The DBE vs. C diagram for 10-18 nm particles is characterized by (1) nine  
465  $C_{18}H_hO_9N_nI$  formulas with DBE = 1-4 and (2)  $C_9H_{16}NO_3I$  and its  $C_{10}$ - $C_{13}$  homologues.  
466 Because these formulas were detected in ESI+ mode, they are most likely iodinated  
467 amino acids. 32-56 nm particles accommodate most abundant iodinated OC formulas,  
468 in terms of both formula number and relative intensity. Prominent formulas include (1)  
469 diiodo acetic acid  $C_2H_2O_2I_2$ , diiodomethane  $CH_2I_2$ , (2) iodinated  $C_{21}$  carbonyls  
470  $C_{21}H_{39}OI$  and  $C_{21}H_{41}OI$ , (3) iodinated  $C_{21,25,27,29}$  alcohols or ethers with DBE = 0, (4)  
471 iodinated  $C_{10}$  and  $C_{15}$  terpene and sesquiterpene oxidation products and (5) iodinated  
472 organic sulfate  $C_8H_{17}N_2SO_8I$  and  $C_{21}H_{43}SO_4I$ . In addition,  $C_9H_{10}NO_3I$  detected in this  
473 size bin (S/N ratio: 35) can be tentatively assigned to an iodinated amino acid  
474 iodotyrosine that has been observed in seaweed (Yang et al., 2016), implying direct  
475 contribution from seaweed emission to new particles.



476 In 180-560 nm particles, the majority of iodinated OC are C<sub>6-9</sub> aromatic CHOI<sup>+</sup>  
477 compounds with AI > 0.5 and DBE = 5-7. Both C and O atom numbers of these  
478 iodinated OC are smaller than those of mono-modally distributed CHO<sup>+</sup> compounds  
479 around C<sub>15</sub> in the same particle size (Figure 3d and S3b). This implies that iodine has a  
480 strong tendency to aromatic compounds in submicron aerosols due to electrophilic  
481 substitution on aromatic rings. In 3.2-5.6 μm particles, iodinated OC features C<sub>4</sub>-C<sub>6</sub>  
482 CHO<sup>+</sup> and CHON<sup>+</sup> compounds with DBE = 3-6, which again have fewer C atoms than  
483 non-iodinated OC. Supporting evidence from AI shows these compounds are not  
484 aromatic. Coastal 3.2-5.6 μm particles can be sea salt particles formed during bubble  
485 bursting of sea water (Russell et al., 2010; Schmitt-Kopplin et al., 2012; Quinn et al.,  
486 2014; Wilson et al., 2015). However, Hao et al. 2017 (Hao et al., 2017) showed that  
487 iodinated OC products from the reaction between iodine and seawater are highly  
488 unsaturated carboxylic-rich polyphenols with DBE = 4-14 and C atoms = 10-30. It is  
489 thus apparent that iodinated OC in 3.2-5.6 μm particles were not directly from iodinated  
490 organic compounds in the seawater.

### 491 **3.5 Atmosphere implications**

492 Due to the 71% ocean coverage of the earth's surface, marine aerosol generation is  
493 important in determining the earth's radiative budget and climate change. Of the limited  
494 number of studies reporting coastal NPF, most have focused on iodine emission,  
495 oxidation and nucleation in the early stage of NPF. In principle, abundant low-volatility  
496 condensing vapors other than iodine are required in coastal environments for the growth  
497 of iodine clusters to CCN. This article reveals a new group of important organics  
498 involved in this process. It is most likely that their precursors are emitted mutually with  
499 iodine from either direct exposure of coastal biota to the atmosphere or biological-active  
500 sea surface. More fundamental field, laboratory and modeling studies are needed to  
501 determine (1) exact emission sources and source rates of these organic precursors, (2)  
502 their gas phase intermediates and oxidation mechanisms in the atmosphere and (3) their  
503 quantitative contribution to global and regional CCN numbers.



504 **ACKNOWLEDGMENTS**

505 The work was supported by the National Science Foundation of China (grant  
506 numbers 41975831 and 41675124) and the National Key Research and Development  
507 Program of China (grant number 2016YFC0203100).

508

509 **Data availability.** The data used in this publication are available from the  
510 corresponding author Huan Yu ([yuhuan@cug.edu.cn](mailto:yuhuan@cug.edu.cn)).

511

512 **Author contributions.** Huan Yu designed and conducted chemical analysis. Yibei  
513 Wan and Huan Yu did data analysis and wrote the paper. Xiangpeng Huang  
514 conducted the field sampling. Bin Jiang and Yuhong Liao did the FT-ICR-MS  
515 analysis. Binyu Kuang, Manfei Lin, Deming Xia, Jingwen Chen and Jianzhen Yu  
516 reviewed and revised the manuscript.

517

518 **Conflict of Interest**

519 The authors declare that they have no conflict of interest.

520

521

522

523 **REFERENCE**

524 Allan, J. D., Williams, P. I., Nájera, J., Whitehead, J. D., Flynn, M. J., Taylor, J. W.,  
525 Liu, D., Darbyshire, E., Carpenter, L. J., Chance, R., Andrews, S. J., Hackenberg, S.  
526 C., and McFiggans, G.: Iodine observed in new particle formation events in the



- 527 Arctic atmosphere during ACCACIA, *Atmos. Chem. Phys.*, 15, 5599-5609,  
528 doi:10.5194/acp-15-5599-2015, 2015.
- 529 An, Y. Q., Xu, J. Z., Feng, L., Zhang, X. H., Liu, Y. M., Kang, S. C., Jiang, B., and  
530 Liao, Y. H.: Molecular characterization of organic aerosol in the Himalayas: insight  
531 from ultra-high-resolution mass spectrometry, *Atmos. Chem. Phys.*, 19, 1115-1128,  
532 doi:10.5194/acp-19-1115-2019, 2019.
- 533 Atkinson, R., Tuazon, E. C., and Aschmann, S. M.: Products of the Gas-Phase  
534 Reactions of a Series of 1-Alkenes and 1-Methylcyclohexene with the OH Radical  
535 in the Presence of NO, *Environ. Sci. Technol.*, 29, 1674-1680,  
536 doi:10.1021/es00006a035, 1995.
- 537 Bao, H. Y., Niggemann, J., Li, L., Dittmar, T., and Kao, S.-J.: Molecular composition  
538 and origin of water-soluble organic matter in marine aerosols in the Pacific off China,  
539 *Atmos. Environ.*, 191, 27-35, doi:10.1016/j.atmosenv.2018.07.059, 2018.
- 540 Barnes, I., Hjorth, J., and Mihalopoulos, N.: Dimethyl Sulfide and Dimethyl Sulfoxide  
541 and Their Oxidation in the Atmosphere, *Chem. Rev.*, 106, 940-975,  
542 doi:10.1021/cr020529+, 2006.
- 543 Barone, S. B., Turnipseed, A. A., and Ravishankara, A. R.: Reaction of OH with  
544 Dimethyl Sulfide (DMS). 1. Equilibrium Constant for OH + DMS Reaction and the  
545 Kinetics of the OH·DMS + O<sub>2</sub> Reaction, *J. Phys. Chem. A.*, 100, 14694-14702,  
546 doi:10.1021/jp960866k, 1996.
- 547 Bianco, A., Deguillaume, L., Vaïtilingom, M., Nicol, E., Baray, J.-L., Chaumerliac, N.,  
548 and Bridoux, M.: Molecular Characterization of Cloud Water Samples Collected at  
549 the Puy de Dôme (France) by Fourier Transform Ion Cyclotron Resonance Mass  
550 Spectrometry, *Environ. Sci. Technol.*, 52, 10275-10285,  
551 doi:10.1021/acs.est.8b01964, 2018.
- 552 Bikkina, P., Kawamura, K., Bikkina, S., Kunwar, B., Tanaka, K., and Suzuki, K.:  
553 Hydroxy Fatty Acids in Remote Marine Aerosols over the Pacific Ocean: Impact of  
554 Biological Activity and Wind Speed, *ACS. Earth. Space. Chem.*, 3, 366-379,  
555 doi:10.1021/acsearthspacechem.8b00161, 2019.
- 556 Blokker, P., Schouten, S., van den Ende, H., De Leeuw, J. W., and Sinninghe Damsté,  
557 J. S.: Cell wall-specific  $\omega$ -hydroxy fatty acids in some freshwater green microalgae,  
558 *Phytochemistry.*, 49, 691-695, doi:10.1016/S0031-9422(98)00229-5, 1998.
- 559 Burkholder, J. B., Curtius, J., Ravishankara, A. R., and Lovejoy, E. R.: Laboratory  
560 studies of the homogeneous nucleation of iodine oxides, *Atmos. Chem. Phys.*, 4, 19-  
561 34, doi:10.5194/acpd-3-4943-2003, 2004.
- 562 Calvert, J. G., Atkinson, R. G., Orlando, J. J., Wallington, T. J., and Tyndall, G. S.: *The  
563 Mechanisms of Atmospheric Oxidation of Alkenes*, Oxford Univ. Press, Oxford, UK.,  
564 2000.
- 565 Cochran, R. E., Laskina, O., Trueblood, J. V., Estillore, A. D., Morris, H. S., Jayarathne,  
566 T., Sultana, C. M., Lee, C., Lin, P., Laskin, J., Laskin, A., Dowling, J. A., Qin, Z.,  
567 Cappa, C. D., Bertram, T. H., Tivanski, A. V., Stone, E. A., Prather, K. A., and  
568 Grassian, V. H.: Molecular Diversity of Sea Spray Aerosol Particles: Impact of  
569 Ocean Biology on Particle Composition and Hygroscopicity, *Chem. Pharm. Bull.*, 2,  
570 655-667, doi:10.1016/j.chempr.2017.03.007, 2017.



- 571 Crounse, J. D., Nielsen, L. B., Jørgensen, S., Kjaergaard, H. G., and Wennberg, P. O.:  
572 Autoxidation of Organic Compounds in the Atmosphere, *J. Phys. Chem. Lett.*, 4,  
573 3513-3520, doi:10.1021/jz4019207, 2013.
- 574 Daellenbach, K. R., Kourtchev, I., Vogel, A. L., Bruns, E. A., Jiang, J. H., Petäjä, T.,  
575 Jaffrezo, J.-L., Aksoyoglu, S., Kalberer, M., Baltensperger, U., Haddad, I. E., and  
576 Prevot, A. S. H.: Impact of anthropogenic and biogenic sources on the seasonal  
577 variation of the molecular composition of urban organic aerosols: a field and  
578 laboratory study using ultra-high resolution mass spectrometry, *Atmos. Chem. Phys.*  
579 *Discuss.*, 19, 5973-5991, doi:10.5194/acp-2018-1128, 2018.
- 580 Dall'Osto, M., Simo, R., Harrison, R. M., Beddows, D. C. S., Saiz-Lopez, A., Lange,  
581 R., Skov, H., Nøjgaard, J. K., Nielsen, I. E., and Massling, A.: Abiotic and biotic  
582 sources influencing spring new particle formation in North East Greenland, *Atmos.*  
583 *Environ.*, 190, 126-134, doi:10.1016/j.atmosenv.2018.07.019, 2018.
- 584 Dawczynski, C., Schubert, R., and Jahreis, G.: Amino acids, fatty acids, and dietary  
585 fibre in edible seaweed products, *Food. Chem.*, 103, 891-899,  
586 doi:10.1016/j.foodchem.2006.09.041, 2007.
- 587 DeMott, P. J., Mason, R. H., McCluskey, C. S., Hill, T. C. J., Perkins, R. J., Desyaterik,  
588 Y., Bertram, A. K., Trueblood, J. V., Grassian, V. H., Qiu, Y., Molinero, V., Tobo,  
589 Y., Sultana, C. M., Lee, C., and Prather, K. A.: Ice nucleation by particles containing  
590 long-chain fatty acids of relevance to freezing by sea spray aerosols, *Environ. Sci-*  
591 *Proc. Imp.*, 20, 1559-1569, doi:10.1039/c8em00386f, 2018.
- 592 Ehn, M., Thornton, J. A., Kleist, E., Sipila, M., Junninen, H., Pullinen, I., Springer, M.,  
593 Rubach, F., Tillmann, R., Lee, B., Lopez-Hilfiker, F., Andres, S., Acir, I. H.,  
594 Rissanen, M., Jokinen, T., Schobesberger, S., Kangasluoma, J., Kontkanen, J.,  
595 Nieminen, T., Kurten, T., Nielsen, L. B., Jørgensen, S., Kjaergaard, H. G.,  
596 Canagaratna, M., Maso, M. D., Berndt, T., Petaja, T., Wahner, A., Kerminen, V. M.,  
597 Kulmala, M., Worsnop, D. R., Wildt, J., and Mentel, T. F.: A large source of low-  
598 volatility secondary organic aerosol, *Nature.*, 506, 476-479,  
599 doi:10.1038/nature13032, 2014.
- 600 Elm, J., Fard, M., Bilde, M., and Mikkelsen, K. V.: Interaction of Glycine with  
601 Common Atmospheric Nucleation Precursors, *J. Phys. Chem. A.*, 117, 12990-12997,  
602 doi:10.1021/jp408962c, 2013.
- 603 Ge, P., Luo, G., Luo, Y., Huang, W., Xie, H. B., Chen, J. W., and Qu, J. P.: Molecular  
604 understanding of the interaction of amino acids with sulfuric acid in the presence of  
605 water and the atmospheric implication, *Chemosphere.*, 210, 215-223,  
606 doi:10.1016/j.chemosphere.2018.07.014, 2018.
- 607 Ge, X. L., Wexler, A. S., and Clegg, S. L.: Atmospheric amines – Part I. A review,  
608 *Atmos. Environ.*, 45, 524-546, doi:10.1016/j.atmosenv.2010.10.012, 2011.
- 609 Gelin, F., Volkman, J. K., De Leeuw, J. W., and Sinninghe Damsté, J. S.: Mid-chain  
610 hydroxy long-chain fatty acids in microalgae from the genus *Nannochloropsis*,  
611 *Phytochemistry.*, 45, 641-646, doi:10.1016/S0031-9422(97)00068-X, 1997.
- 612 Guo, Z. G., Sheng, L. F., Feng, J. L., and Fang, M.: Seasonal variation of solvent  
613 extractable organic compounds in the aerosols in Qingdao, China, *Atmos. Environ.*,  
614 37, 1825-1834, doi:10.1016/S1352-2310(03)00064-5, 2003.





- 615 Hao, Z. N., Yin, Y. G., Cao, D., and Liu, J. F.: Probing and Comparing the  
616 Photobromination and Photoiodination of Dissolved Organic Matter by Using Ultra-  
617 High-Resolution Mass Spectrometry, *Environ. Sci. Technol.*, 51, 5464-5472,  
618 doi:10.1021/acs.est.6b03887, 2017.
- 619 Ishijima, H., Uchida, R., Ohtawa, M., Kondo, A., Nagai, K., Shima, K., Nonaka, K.,  
620 Masuma, R., Iwamoto, S., Onodera, H., Nagamitsu, T., and Tomoda, H.:  
621 Simplifungin and Valsafungins, Antifungal Antibiotics of Fungal Origin, *J. Org.*  
622 *Chem.*, 81, 7373-7383, doi:10.1021/acs.joc.6b00952, 2016.
- 623 Jares-Erijman, E. A., Bapat, C. P., Lithgow-Bertelloni, A., Rinehart, K. L., and Sakai,  
624 R.: Crucigasterins, new polyunsaturated amino alcohols from the mediterranean  
625 tunicate *Pseudodistoma crucigaster*, *J. Org. Chem.*, 58, 5732-5737,  
626 doi:10.1021/jo00073a036, 1993.
- 627 Jen, C. N., McMurry, P. H., and Hanson, D. R.: Stabilization of Sulfuric Acid Dimers  
628 by Ammonia, Methylamine, Dimethylamine, and Trimethylamine, *J. Geophys. Res-*  
629 *Atmos.*, 119, 7502-7514, doi:10.1002/2014JD021592, 2014.
- 630 Jiang, B., Kuang, B. Y., Liang, Y. M., Zhang, J. Y., Huang, X. H. H., Xu, C. M., Yu,  
631 J., and Shi, Q.: Molecular composition of urban organic aerosols on clear and hazy  
632 days in Beijing: A comparative study using FT-ICR MS, *Environ. Chem.*, 13, 888-  
633 901, doi:10.1071/EN15230, 2016.
- 634 Kendel, M., Barnathan, G., Fleurence, J., Rabesaotra, V., and Wielgosz-Collin, G.:  
635 Non-methylene Interrupted and Hydroxy Fatty Acids in Polar Lipids of the Alga  
636 *Grateloupia turuturu* Over the Four Seasons, *Lipids.*, 48, 535-545,  
637 doi:10.1007/s11745-013-3783-5, 2013.
- 638 Kim, K. R., and Oh, D. K.: Production of hydroxy fatty acids by microbial fatty acid-  
639 hydroxylation enzymes, *Biotechnol. Adv.*, 31, 1473-1485,  
640 doi:10.1016/j.biotechadv.2013.07.004, 2013.
- 641 Kourtchev, I., Fuller, S., Aalto, J., Ruuskanen, T. M., McLeod, M. W., Maenhaut, W.,  
642 Jones, R., Kulmala, M., and Kalberer, M.: Molecular composition of boreal forest  
643 aerosol from Hyytiälä, Finland, using ultrahigh resolution mass spectrometry,  
644 *Environ. Sci. Technol.*, 47, 4069-4079, doi:10.1021/es3051636, 2013.
- 645 Kumar, M., Saiz-Lopez, A., and Francisco, J. S.: Single-Molecule Catalysis Revealed:  
646 Elucidating the Mechanistic Framework for the Formation and Growth of  
647 Atmospheric Iodine Oxide Aerosols in Gas-Phase and Aqueous Surface  
648 Environments, *J. Am. Chem. Soc.*, 140, 14704-14716, 10.1021/jacs.8b07441, 2018.
- 649 Kurtén, T., Loukonen, V., Vehkamäki, H., and Kulmala, M.: Amines are likely to  
650 enhance neutral and ion-induced sulfuric acid-water nucleation in the atmosphere  
651 more effectively than ammonia, *Atmos. Chem. Phys.*, 8, 7455-7476,  
652 doi:10.5194/acpd-8-7455-2008, 2008.
- 653 Li, D. F., Chen, D. P., Liu, F. Y., and Wang, W. L.: Role of glycine on sulfuric acid-  
654 ammonia clusters formation: Transporter or participator, *J. Environ. Sci.*, 89, 125-  
655 135, doi:10.1016/j.jes.2019.10.009, 2020.
- 656 Lin, P., Rincon, A. G., Kalberer, M., and Yu, J. Z.: Elemental Composition of HULIS  
657 in the Pearl River Delta Region, China: Results Inferred from Positive and Negative



- 658 Electrospray High Resolution Mass Spectrometric Data, *Environ. Sci. Technol.*, 46,  
659 7454-7462, doi:10.1021/es300285d, 2012.
- 660 Litchfield, C., Greenberg, A. J., Noto, G., and Morales, R. W.: Unusually high levels  
661 of C<sub>24</sub>–C<sub>30</sub> fatty acids in sponges of the class demospongiae, *Lipids.*, 11, 567-570,  
662 doi:10.1007/BF02532903, 1976.
- 663 Mahajan, A. S., Sorribas, M., Martín, J. C. G., MacDonald, S. M., Gil, M., Plane, J. M.  
664 C., and Saiz-Lopez, A.: Concurrent observations of atomic iodine, molecular iodine  
665 and ultrafine particles in a coastal environment, *Atmos. Chem. Phys. Discuss.*, 11,  
666 2545-2555, doi:10.5194/acp-11-2545-2011, 2010.
- 667 Mansour, M. P., Volkman, J. K., Holdsworth, D. G., Jackson, A. E., and Blackburn, S.  
668 I.: Very-long-chain (C<sub>28</sub>) highly unsaturated fatty acids in marine dinoflagellates,  
669 *Phytochemistry.*, 50, 541-548, doi:10.1016/S0031-9422(98)00564-0, 1999.
- 670 Mazzoleni, L. R., Saranjampour, P., Dalbec, M. M., Samburova, V., Hallar, G. A.,  
671 Zielinska, B., Lowenthal, D. H., and Kohl, S.: Identification of water-soluble organic  
672 carbon in non-urban aerosols using ultrahigh-resolution FT-ICR mass spectrometry:  
673 Organic anions, *Environ. Chem.*, 9, 285-297, doi:10.1071/EN11167, 2012.
- 674 Mentel, T. F., Springer, M., Ehn, M., Kleist, E., Pullinen, I., Kurtén, T., Rissanen, M.,  
675 Wahner, A., and Wildt, J.: Formation of highly oxidized multifunctional compounds:  
676 autoxidation of peroxy radicals formed in the ozonolysis of alkenes – deduced from  
677 structure–product relationships, *Atmos. Chem. Phys.*, 15, 6745-6765,  
678 doi:10.5194/acp-15-6745-2015, 2015.
- 679 Merikanto, J., Spracklen, D. V., Mann, G. W., Pickering, S. J., and Carslaw, K. S.:  
680 Impact of nucleation on global CCN, *Atmos. Chem. Phys.*, 9, 12999–13037,  
681 doi:10.5194/acp-9-8601-2009, 2009.
- 682 Metzger, A., Verheggen, B., Dommen, J., Duplissy, J., Prevot, A. S. H., Weingartner,  
683 E., Riipinen, I., Kulmala, M., Spracklen, D. V., Carslaw, K. S., and Baltensperger,  
684 U.: Evidence for the role of organics in aerosol particle formation under atmospheric  
685 conditions, *Proc. Natl. Acad. Sci. U. S. A.*, 107, 6646-6651,  
686 doi:10.1073/pnas.0911330107, 2010.
- 687 Moss, G. P., Smith, P. A. S., and Tavernier, D.: Glossary of class names of organic  
688 compounds and reactivity intermediates based on structure (IUPAC  
689 Recommendations 1995), *pac*, 67, 1307-1375, doi:10.1351/pac199567081307, 1995.
- 690 Ning, C. P., Gao, Y., Zhang, H. J., Yu, H. R., Wang, L., Geng, N. B., Cao, R., and Chen,  
691 J. P.: Molecular characterization of dissolved organic matters in winter atmospheric  
692 fine particulate matters (PM<sub>2.5</sub>) from a coastal city of northeast China, *Sci. Total.  
693 Environ.*, 689, 312-321, doi:10.1016/j.scitotenv.2019.06.418, 2019.
- 694 O'Dowd, C. D., Jimenez, J. L., Bahreini, R., Flagan, R. C., Seinfeld, J. H., Hämeri, K.,  
695 Pirjola, L., Kulmala, M., Jennings, S. G., and Hoffmann, T.: Marine aerosol  
696 formation from biogenic iodine emissions, *Nature.*, 417, 632-636,  
697 doi:10.1038/nature00775, 2002.
- 698 Pankow, J. F., and Asher, W. E.: SIMPOL.1: a simple group contribution method for  
699 predicting vapor pressures and enthalpies of vaporization of multifunctional organic  
700 compounds, *Atmos. Chem. Phys.*, 8, 2773-2796, doi:10.5194/acp-8-2773-2008,  
701 2008.



- 702 Pollard, M., Beisson, F., Li, Y., and Ohlogge, J. B.: Building lipid barriers:  
703 biosynthesis of cutin and suberin, *Trends. Plant. Sci.*, 13, 236-246,  
704 doi:10.1016/j.tplants.2008.03.003, 2008.
- 705 Pratt, K. A., and Prather, K. A.: Mass spectrometry of atmospheric aerosols--recent  
706 developments and applications. Part I: Off-line mass spectrometry techniques, *Mass.*  
707 *Spectrom. Rev.*, 31, 1-16, doi:10.1002/mas.20322, 2012.
- 708 Quinn, P. K., Bates, T. S., Schulz, K. S., Coffman, D. J., Frossard, A. A., Russell, L.  
709 M., Keene, W. C., and Kieber, D. J.: Contribution of sea surface carbon pool to  
710 organic matter enrichment in sea spray aerosol, *Nat. Geosci.*, 7, 228-232,  
711 doi:10.1038/ngeo2092, 2014.
- 712 Řezanka, T., and Podojil, M.: The very long chain fatty acids of the green alga, *Chlorella*  
713 *kessleri*, *Lipids.*, 19, 472, doi:10.1007/BF02537412, 1984.
- 714 Richters, S., Herrmann, H., and Berndt, T.: Highly Oxidized RO<sub>2</sub> Radicals and  
715 Consecutive Products from the Ozonolysis of Three Sesquiterpenes, *Environ. Sci.*  
716 *Technol.*, 50, 2354-2362, doi:10.1021/acs.est.5b05321, 2016.
- 717 Rogge, W. F., Hildemann, L. M., Mazurek, M. A., Cass, G. R., and Simoneit, B. R. T.:  
718 Sources of fine organic aerosol. 1. Charbroilers and meat cooking operations,  
719 *Environ. Sci. Technol.*, 25, 1112-1125, doi:10.1021/es00018a015, 1991.
- 720 Roscoe, H. K., Jones, A. E., Brough, N., Weller, R., Saiz-Lopez, A., Mahajan, A. S.,  
721 Schoenhardt, A., Burrows, J. P., and Fleming, Z. L.: Particles and iodine compounds  
722 in coastal Antarctica, *J. Geophys. Res-Atmos.*, 120, 7144-7156,  
723 doi:10.1002/2015JD023301, 2015.
- 724 Russell, L. M., Hawkins, L. N., Frossard, A. A., Quinn, P. K., and Bates, T. S.:  
725 Carbohydrate-like composition of submicron atmospheric particles and their  
726 production from ocean bubble bursting, *Proc. Natl. Acad. Sci. U. S. A.*, 107, 6652,  
727 doi:10.1073/pnas.0908905107, 2010.
- 728 Saiz-Lopez, A., Plane, J. M. C., Baker, A. R., Carpenter, L. J., von Glasow, R., Gómez  
729 Martín, J. C., McFiggans, G., and Saunders, R. W.: Atmospheric Chemistry of Iodine,  
730 *Chem. Rev.*, 112, 1773-1804, doi:10.1021/cr200029u, 2012.
- 731 Schmitt-Kopplin, P., Liger-Belair, G., Koch, B. P., Flerus, R., Kattner, G., Harir, M.,  
732 Kanawati, B., Lucio, M., Tziotis, D., Hertkorn, N., and Gebefügi, I.: Dissolved  
733 organic matter in sea spray: a transfer study from marine surface water to aerosols,  
734 *Biogeosciences.*, 9, 1571-1582, doi:10.5194/bg-9-1571-2012, 2012.
- 735 Schum, S. K., Zhang, B., Džepina, K., Fialho, P., Mazzoleni, C., and Mazzoleni, L. R.:  
736 Molecular and physical characteristics of aerosol at a remote free troposphere site:  
737 implications for atmospheric aging, *Atmos. Chem. Phys.*, 18, 14017-14036,  
738 doi:10.5194/acp-18-14017-2018, 2018.
- 739 Simoneit, B. R. T., and Mazurek, M. A.: Organic matter of the troposphere—II.\*\*For  
740 Part I, see Simoneit et al. (1977). Natural background of biogenic lipid matter in  
741 aerosols over the rural western united states, *Atmos. Environ.*, 16, 2139-2159,  
742 doi:10.1016/0004-6981(82)90284-0, 1982.
- 743 Sipilä, M., Sarnela, N., Jokinen, T., Henschel, H., Junninen, H., Kontkanen, J., Richters,  
744 S., Kangasluoma, J., Franchin, A., Peräkylä, O., Rissanen, M. P., Ehn, M.,  
745 Vehkamäki, H., Kurten, T., Berndt, T., Petäjä, T., Worsnop, D., Ceburnis, D.,



- 746 Kerminen, V.-M., Kulmala, M., and O'Dowd, C.: Molecular-scale evidence of  
747 aerosol particle formation via sequential addition of HIO<sub>3</sub>, *Nature.*, 537, 532-534,  
748 doi:10.1038/nature19314, 2016.
- 749 Stevanović, K. Z., Bubanja, I. N. M., and Stanisavljev, D. R.: Is Iodine Oxidation with  
750 Hydrogen Peroxide Coupled with Nucleation Processes?, *J. Phys. Chem. C.*, 123,  
751 16671-16680, doi:10.1021/acs.jpcc.9b02563, 2019.
- 752 Tsukamoto, D., Shibano, M., and Kusano, G.: Studies on the Constituents of  
753 Broussonetia Species X. Six New Alkaloids from Broussonetia kazinoki SIEB,  
754 *Chem. Pharm. Bull.*, 49, 1487-1491, doi:10.1248/cpb.49.1487, 2001.
- 755 VanMiddlesworth, F., Giacobbe, R. A., Lopez, M., Garrity, G., Bland, J., Bartizal, K.,  
756 Fromtling, R. A., Polishook, J., Zweerink, M., and Edison, A. M.: Sphingofungins  
757 A, B, C, and D; a new family of antifungal agents. I. Fermentation, isolation, and  
758 biological activity, *J. Antibiot.*, 45, 861-867, 1992.
- 759 Vereecken, L., Glowacki, D. R., and Pilling, M. J.: Theoretical Chemical Kinetics in  
760 Tropospheric Chemistry: Methodologies and Applications, *Chem. Rev.*, 115, 4063-  
761 4114, doi:10.1021/cr500488p, 2015.
- 762 Volkman, J. K., Barrett, S. M., Dunstan, G. A., and Jeffrey, S. W.: C30-C32 alkyl diols  
763 and unsaturated alcohols in microalgae of the class Eustigmatophyceae, *Org.*  
764 *Geochem.*, 18, 131-138, doi:10.1016/0146-6380(92)90150-V, 1992.
- 765 Willoughby, A. S., Wozniak, A. S., and Hatcher, P. G.: Detailed Source-Specific  
766 Molecular Composition of Ambient Aerosol Organic Matter Using Ultrahigh  
767 Resolution Mass Spectrometry and <sup>1</sup>H NMR, *Atmosphere.*, 7, 79,  
768 doi:10.3390/atmos7060079, 2016.
- 769 Wilson, T. W., Ladino, L. A., Alpert, P. A., Breckels, M. N., Brooks, I. M., Browse, J.,  
770 Burrows, S. M., Carslaw, K. S., Huffman, J. A., Judd, C., Kilhau, W. P., Mason, R.  
771 H., McFiggans, G., Miller, L. A., Nájera, J. J., Polishchuk, E., Rae, S., Schiller, C.  
772 L., Si, M., Temprado, J. V., Whale, T. F., Wong, J. P. S., Wurl, O., Yakobi-Hancock,  
773 J. D., Abbatt, J. P. D., Aller, J. Y., Bertram, A. K., Knopf, D. A., and Murray, B. J.:  
774 A marine biogenic source of atmospheric ice-nucleating particles, *Nature.*, 525, 234-  
775 238, doi:10.1038/nature14986, 2015.
- 776 Wu, C. H., Yang, J., Fu, Q., Zhu, B., Ruan, T., and Jiang, G. B.: Molecular  
777 characterization of water-soluble organic compounds in PM<sub>2.5</sub> using ultrahigh  
778 resolution mass spectrometry, *Sci. Total. Environ.*, 668, 917-924,  
779 doi:10.1016/j.scitotenv.2019.03.031, 2019.
- 780 Xie, Q. R., Su, S. H., Chen, S., Xu, Y. S., Cao, D., Chen, J., Ren, L. J., Yue, S. Y., Zhao,  
781 W. Y., Sun, Y. L., Wang, Z. F., Tong, H. J., Su, H., Cheng, Y. F., Kawamura, K.,  
782 Jiang, G. B., Liu, C. Q., and Fu, P. Q.: Molecular Characterization of Firework-  
783 Related Urban Aerosols using FT-ICR Mass Spectrometry, *Atmos. Chem. Phys.*, 1-  
784 29, 10.5194/acp-2019-1180, 2020.
- 785 Yang, Y. J., Peng, Y. E., Chang, Q., Dan, C. H., Guo, W., and Wang, Y. X.: Selective  
786 Identification of Organic Iodine Compounds Using Liquid Chromatography–High  
787 Resolution Mass Spectrometry, *Anal. Chem.*, 88, 1275-1280,  
788 doi:10.1021/acs.analchem.5b03694, 2016.



- 789 Yao, L., Wang, M. Y., Wang, X. K., Liu, Y. J., Chen, H. F., Zheng, J., Nie, W., Ding,  
790 A. J., Geng, F. H., Wang, D. F., Chen, J. M., Worsnop, D. R., and Wang, L.:  
791 Detection of atmospheric gaseous amines and amides by a high-resolution time-of-  
792 flight chemical ionization mass spectrometer with protonated ethanol reagent ions,  
793 *Atmos. Chem. Phys.*, 16, 14527-14543, doi:10.5194/acp-16-14527-2016, 2016.
- 794 Yassine, M. M., Harir, M., Dabek, E., and Schmitt-Kopplin, P.: Structural  
795 characterization of organic aerosol using Fourier transform ion cyclotron resonance  
796 mass spectrometry: Aromaticity equivalent approach, *Rapid. Commun. Mass. Sp.*,  
797 28, 2445-2454, doi:10.1002/rcm.7038, 2014.
- 798 Yoon, Y. J., O'Dowd, C. D., Jennings, S. G., and Lee, S. H.: Statistical characteristics  
799 and predictability of particle formation events at Mace Head, *J. Geophys. Res.*, 111,  
800 D13204, doi:10.1029/2005JD006284, 2006.
- 801 Yu, H., Ren, L. L., Huang, X. P., Xie, M. J., He, J., and Xiao, H.: Iodine speciation and  
802 size distribution in ambient aerosols at a coastal new particle formation hotspot in  
803 China, *Atmos. Chem. Phys.*, 19, 4025-4039, doi:10.5194/acp-19-4025-2019, 2019.
- 804 Yvon, S. A., Saltzman, E. S., Cooper, D. J., Bates, T. S., and Thompson, A. M.:  
805 Atmospheric sulfur cycling in the tropical Pacific marine boundary layer (12°S,  
806 135°W): A comparison of field data and model results: 1. Dimethylsulfide, *J.*  
807 *Geophys. Res-Atmos.*, 101, 6899-6909, doi:10.1029/95JD03356, 1996.
- 808 Zhao, Y., Hallar, A. G., and Mazzoleni, L. R.: Atmospheric organic matter in clouds:  
809 exact masses and molecular formula identification using ultrahigh-resolution FT-  
810 ICR mass spectrometry, *Atmos. Chem. Phys.*, 13, 12343-12362, doi:10.5194/acp-  
811 13-12343-2013, 2013.
- 812 Zheng, M., Fang, M., Wang, F., and To, K. L.: Characterization of the solvent  
813 extractable organic compounds in PM<sub>2.5</sub> aerosols in Hong Kong, *Atmos. Environ.*,  
814 34, 2691-2702, doi:10.1016/S1352-2310(99)00521-X, 2000.
- 815 Zuth, C., Vogel, A. L., Ockenfeld, S., Huesmann, R., and Hoffmann, T.: Ultrahigh-  
816 Resolution Mass Spectrometry in Real Time: Atmospheric Pressure Chemical  
817 Ionization Orbitrap Mass Spectrometry of Atmospheric Organic Aerosol, *Anal.*  
818 *Chem.*, 90, 8816-8823, doi:10.1021/acs.analchem.8b00671, 2018.
- 819